

## Electronic Structure and Properties of Metal Ti/Insulator MgO Superlattice

Kenji Koga, Koji Akai, Kazunori Ohsiro, Tetsuo Kado\*, Hiroaki Anno\*\* and Mitsuru Matsuura  
Faculty of Engineering, Yamaguchi University, 2-16-1, Tokiwadai, Ube, Yamaguchi 755-8611, JAPAN

Fax: 81-0836-85-9622, e-mail: b5229@yamaguchi-u.ac.jp

\*The National Institute of Advanced Industrial Science and Technology, Chugoku, MITI, 2-2-2, Hiro-Suehiro,  
Kure, Hiroshima, 737-01, JAPAN

\*\*Department of Electronics and Computer Science, Science University of Tokyo in Yamaguchi, 1-1-1 Daigaku-Dohri, Onoda  
756-0884, JAPAN

Electronic structure of metal Ti/insulator MgO superlattice is calculated by the full potential linearized augmented plane wave (FLAPW) with the generalized gradient approximation (GGA) and the inclusion of the spin-orbit interaction. It is found that there are two kinds of electronic state; (i) one is the state that extends to the both Ti and MgO layers and have a dispersion in the  $k$ -direction reflecting the growth direction of the superlattice. (ii) The other is the state that occupies only one of the Ti or MgO layers and has little dispersion; then, the state constitutes the quasi two-dimensional electronic state in each layer. Electronic states near Fermi level consist of metallic states in a Ti layer that lay within the band gap in an insulator MgO layer. Based on the electronic structure calculation, band diagram of Ti/MgO superlattices is presented. X-ray photoelectron spectra are measured and a good correspondence is obtained with the calculated density of states in the conduction and valence electron region. X-ray absorption and emission spectra are also calculated.

Key words: metal/insulator superlattice, FLAPW, electronic structure, band diagram

### 1. INTRODUCTION

The semiconductor superlattice has been studied very much both on basic physical properties and on the application to electronic devices. On the other hand, only a few studies have been done in metal/insulator superlattice; in metal/insulator superlattice systems electronic states in a metallic layer are expected to become those of a quasi-two dimensional metal, since electrons confined in the layer by the high potential barrier of the insulator. By varying well and barrier width, electronic structures and transport properties of a superlattice are controlled. Thus, experimental research in  $\text{CoSi}_2/\text{CaF}_2$  and Ti/MgO has been performed mainly for device application, but basic physical property in these systems has been studied little [1-7]. Considering high electronic concentration in these systems compared with that in the semiconductor superlattice, it may be possible to develop quantum electronic devices, such as transistors and diodes, which result in the improvement in the speed of an element, or integration.

In the experimental side Watanabe *et al.*, prepared the resonant tunneling diode by using  $\text{CoSi}_2/\text{CaF}_2$  superlattice system, and have succeeded in the confirmation of the current amplification operation and hot electron transistor of the negative resistance, which is based on the quantum resonant tunnel transport [1-2]. Also one of present author has succeeded in the preparation of Ag/NiO and Ti/MgO superlattices by molecular beam epitaxy (MBE) [4-6].

In theoretical side some of our group have performed the first calculation of the electronic

structure of metal/insulator superlattice; calculation has been done for  $\text{CoSi}_2/\text{CaF}_2$  system and features such as confinement of electronics states in each layers are clarified [3]. In addition, recently the theoretical analysis of the tunneling current has been made [7].

It is important to study the basic physical properties of the system such as electronic structure of the metal/insulator superlattice, which yields the band discontinuities being important for the development in electronic device. In the present study, electronic structure of the Ti/MgO superlattice is presented; we use FLAPW (full-potential linearized augmented plane wave) method, based on density functional theory with the inclusion of the spin-orbit interaction.

### 2. CRYSTAL STRUCTURE OF METAL Ti/INSULATOR MgO

Here we briefly introduce the structure of Ti/MgO superlattice, which were grown on a MgO (001) substrates by the MBE [4]. The crystal structure has been determined by the X-ray diffraction (XRD) technique. Ti and MgO layers were grown alternatively for 25 periods on the buffer layer in  $10^{-7}$  Pa atmospheres. The structure was determined by the low angle and middle angle XRD measurements. The thicknesses of Ti and MgO layers have been identified from the low angle measurement, 9.77 Å (Ti) and 8.37 Å (MgO) respectively. The interplanar spacings of Ti and MgO in the growth direction were estimated to be 2.03 Å and 2.15 Å, and Ti and MgO layers in the superlattice consist of the 3.9 MgO and 4.8 Ti molecular (atomic)

layers in an average from the medium angle XRD measurement. From these results, it is considered that Ti layer have the face centered tetragonal (fct) structure with the lattice constant  $a_0=b_0=4.17 \text{ \AA}$ ,  $c_0=4.06 \text{ \AA}$ , and MgO layer have tetragonal NaCl structure with the lattice constant  $a_0=b_0=4.17 \text{ \AA}$ ,  $c_0=4.29 \text{ \AA}$ . The crystal structure of the superlattice becomes the periodic structure of fct-Ti and fct-MgO layers.

However on the atomic positions of Ti and MgO layer interface there is no information from the experiment. Thus, the atomic configuration in the superlattice interface is determined theoretically from the comparison of the calculated total energies. The calculated result, by the same method as in the calculation of electronic structure described in the following sec.3.1, shows that the Ti atom is in contact with the O atom at the interface. Based on this atomic configuration at the interface, electronic band structure of the superlattice is calculated in the following.

### 3. ELECTRONIC STRUCTURE

#### 3.1 Method of calculation

The electronic structure was computed by solving the Kohn-Sham equation including spin-orbit (SO) interaction with the FLAPW method. Electronic potential is constructed by the density functional (DF) method: the exchange-correlation energy is calculated by using the Perdew-Burke-Ernzerhof expression [8]. In the self-consistent calculation for  $(\text{Ti})_9/(\text{MgO})_5$  superlattice 132 k-sampling points are taken in an

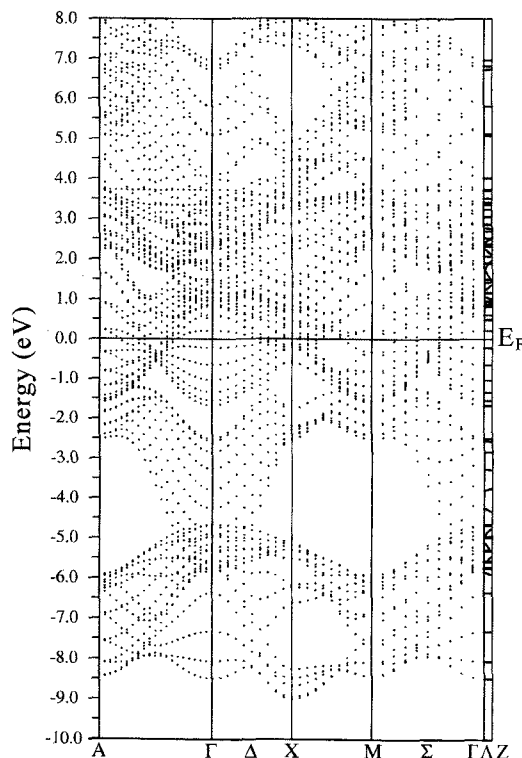


Fig.1 The calculated band structure of  $(\text{Ti})_9/(\text{MgO})_5$  superlattice.

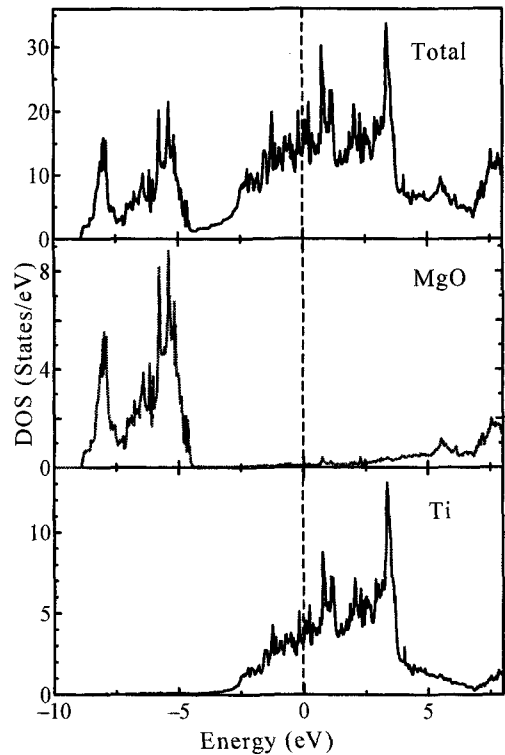


Fig.2 The total and atomic-decomposed densities of states the in Ti/MgO superlattice.

irreducible Brillouin zone (BZ), and about 2000 plane waves were used for constructing APWs. Radii of muffin-tin spheres are chosen as 2.2 a.u. (Ti, Mg) and 2.0 a.u. (O). The matrix elements for the SO Hamiltonian have been neglected when the energy difference between two states is larger than 5Ry.

#### 3.2. Results and discussion

The band structure of  $(\text{Ti})_9/(\text{MgO})_5$  superlattice, i.e., the periodic structure of 9-layer Ti and 5-layer MgO, is shown in Fig.1. The density of states (DOS) of Ti/MgO superlattice is calculated from the band structure and is shown in Fig.2. We have also looked into the wavefunctions to see the character, i.e., the atomic origin of the various bands; electronic states consist of (i) s and p-like states of MgO in the region between -9 and -6 eV, (ii) sp-like states of MgO and mainly of Ti s-like state are mixed in the region between -6 and -5 eV, (iii) mainly d-like states mixed with s and p-like states of Ti in the region between -5 and 1 eV, and (iv) sp-like states of MgO and mainly d-like states of Ti are mixed in the region between 1 and 4 eV.

We notice some features in the results in Figs.1 and 2. Firstly, as seen in Fig.1, there are the Fermi level crossing bands and then the Ti/MgO superlattice is a metal. Secondly in the direction of  $\Lambda$  axis the flat band appears in the energy region between -4 and 1 eV, whose states are confined in Ti layer. In this energy region there exist mainly d-like states mixed with sp-like

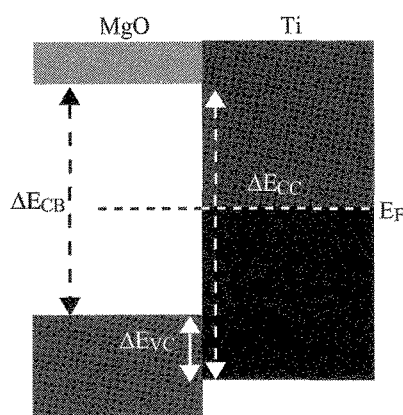


Fig.3 The band diagram of Ti/MgO superlattice

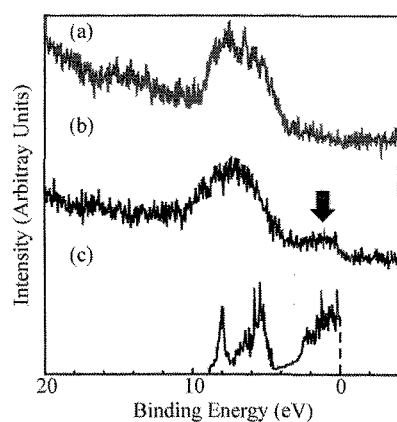


Fig.4 Valence band X-ray photoelectron spectra (XPS) for Ti/MgO superlattice (a) with no etching, (b) with etching in 7 minutes. (c) the density of states below the Fermi energy of Ti/MgO calculated by FLAPW method.

states of Ti and bands have parabolic nature in the  $k_x$ - $k_y$  plane. If we see both Fig.1 and Fig.2 together, we can see MgO layer has the band gap in the energy region between -4 and 1 eV. Furthermore in this region there are electronic states confined in Ti layer. Therefore, the one-dimensional quantum well is formed for the electron in Ti layers. There is also the flat band between -9 and -6 eV, where states are confined in the MgO layer instead of Ti layer and have also the parabolic nature in the  $k_x$ - $k_y$  plane. Thirdly, as seen in Fig.1 and 2 there is another type of electronic states, which have electron distribution in both Ti and MgO layers, and have a dispersion in the direction of  $\Lambda$  axis in the energy region between -6 and -5 eV below the Fermi energy and between 1 and 4 eV above the Fermi energy where sp-like states of MgO and mainly s-like or d-like states of Ti are mixed.

Therefore, there are two kinds of electronic state; one is the state that extends to the both Ti and MgO layers and have a dispersion in the  $k$ -direction reflecting the growth direction of the superlattice. The other is the state that is confined to only one of the Ti or MgO layers and has little dispersion; then, the state is considered to

constitute the quasi two-dimensional electronic state in the  $k_x$ - $k_y$  plane.

#### 4. BAND DISCONTINUITY

The physical property of the superlattice is affected much by the band discontinuity, which is shown in the band diagram of the  $(\text{Ti})_9/(\text{MgO})_5$  superlattice in Fig.3. Here, the band diagram of the Ti/MgO superlattice has been obtained from the present first-principle electronic calculation as follows [9]. It is well known that the density functional (DF) method can describe the ground state well. However good results for the excited state such as the energy position of the conduction bands, i.e., the band gap are not obtained; smaller band gap is resulted. Actually we calculate the band gap in bulk MgO (fcc) by the same method as in sec. 2: obtained result is 4.74 eV at the  $\Gamma$  point. On the other hand, the experimental band gap of MgO is 7.76 eV at the  $\Gamma$  point. The calculated band gap is about 2/3 of the experimental value. Then, using the experimental value for the band gap of MgO, i.e.,  $\Delta E_{CB}=7.76$  eV, the band diagram is constructed and is shown in Fig.3. Here, from the first principle band calculation energy difference between the bottoms of conduction band in Ti and the top of valence band in MgO was calculated to be  $\Delta E_{VC}=1.14$  eV. Therefore the value  $\Delta E_{CC}=8.90$  eV is obtained for the energy difference between bottoms of conduction bands in MgO layer and Ti layer.

#### 5. XPS MEASUREMENT

For the metal Ti/insulator MgO superlattice sample introduced in the sec. 2, X-ray photoelectron spectroscopy (XPS) measurement was performed by using a Shimadzu AXIS-HS systems consisting of ultrahigh vacuum chamber (a base pressure:  $10^{-8}$  Pa) and a load-lock system. The results are shown in Fig.4. Fig.4 shows the X-ray photoelectron spectra for Ti/MgO superlattice (a) with no etching and (b) with etching in 7 minutes. For comparison the calculated density of states below the Fermi energy is also shown in curve Fig.4 (c).

XPS reflects the occupied states, i.e., the states below the Fermi energy in the density of states: main peak structures in Fig.4 (c) consist of s, p-like states of MgO in the binding energy region between 9 and 5 eV and d-like states mixed with s, p-like states of Ti in the binding energy region 5 and 0 eV. Considering these points the spectrum Fig.4 (a) and (b) are considered as follows. In the spectrum before the etching, i.e., in the spectrum Fig.4 (a), only the peak due to MgO, which is the top layer of the superlattice sample, appears, and the peak due to Ti near the Fermi surface is not seen. In the spectra after the etching, the small peak due to Ti indicated by the downward arrow appears as shown in Fig.4 (b). Calculated density of states agrees reasonably well with experimental spectra. Relative magnitude of the

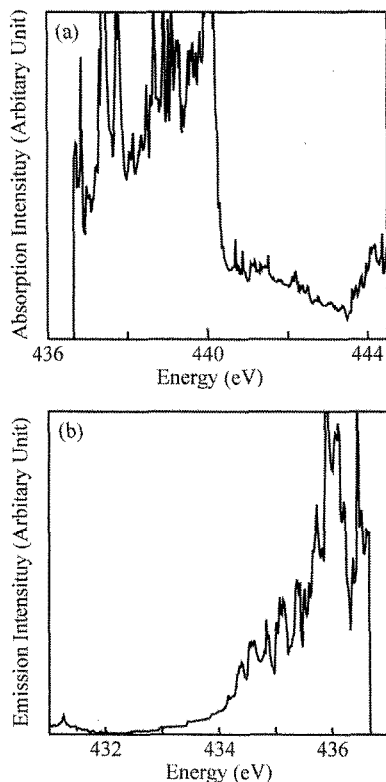


Fig.5 Calculated Ti  $L_{III}$  X-ray (a) absorption and (b) emission spectra of Ti/MgO.

both peaks may change for the duration of the etching time.

## 6. X-RAY ABSORPTION AND EMISSION

X-ray absorption and emission spectra of Ti/MgO superlattice are calculated. X-ray absorption and emission spectra at the near edge reflect a partial DOS of each atomic orbital for electronic states. Thus these spectra yield the good the reliability test for the electronic structure calculation. The cross-section of X-ray absorption within a dipole approximation is given as [10];

$$\sigma_{\text{abs}}(\omega) = 4\pi^2\alpha\omega \sum_{nk} \sum_{imj} N_i |\hat{\epsilon} \cdot \langle nk | \hat{r} | imj \rangle|^2 \delta(\hbar\omega - \varepsilon_{nk} + \varepsilon_{imj}),$$

where  $\varepsilon_{nk}$  is the energy of a conduction electron with the  $n$ -th band and the wave vector  $k$ ,  $\varepsilon_{imj}$  is energy of a core state, characterized by the primary index  $m$  and total angular momentum  $j$  at an  $i$ -atom.  $N_i$  is the number of  $i$ -atom, and  $\alpha$  is fine-structure constant. As low-energy core states (K, L, M,) are localized in the muffin-tin (MT) sphere, integral of the  $\langle nk | \hat{r} | imj \rangle$  is restricted in a MT sphere.

The calculated result for the X-ray (a) absorption and (b) emission spectra are shown in Fig.5. The absorption spectrum reflects the electronic states above the Fermi level in the conduction electron region, which are the final states for transition from the initial core states in the absorption. Due to the dipole matrix element

$\langle nk | \hat{r} | imj \rangle$ , the spectrum Fig.5 (a) has two types of transition process: (i) Ti core 2p state - 3d character conduction electron states transition and (ii) Ti core 2p state - 4s character conduction electron states transition. Actually the spectrum Fig.5 (b) reflects the final states of mainly d character states of Ti, in the energy region between 436.5 and 440.5 eV.

The X-ray emission spectrum reflects the conduction electronic structure below the Fermi level for the initial state in emission process. The spectrum in Fig.5 (b) has two types of transition process as in the absorption: Ti 3d like character conduction states - 2p core state transition and Ti 4s like character conduction states - 2p core state transition. In the energy region between 434.0 and 436.5 eV of the spectrum in Fig.5 (b) reflects the initial states of mainly d character conduction states. However in the lower energy region below 434 eV, the spectrum reflects mainly s character states of Ti as the initial state: there quasi-two dimensional character of the band appears. The present calculated X-ray optical spectra may be used for the reliability test of the electronic structure calculation by the experiment.

## 8. Conclusion

Results of the present electronic structure calculation of Ti/MgO superlattice shows that (i) there are metallic electronic states in a Ti layer within the band gap in an insulator MgO layer and (ii) in the energy region where electronic states exists only in the one of the layer, the states receive the quantum confinement effects and then, quasi two-dimensional character appears. XPS measurement for this system has been performed and a reasonable agreement is obtained with the calculated density of states. X-ray optical spectra of Ti/MgO superlattice are also calculated and the result will be used for the reliability test by the future experiment.

## References

- [1] T. Suemasu, M. Watanabe, J. Suzuki, Kohno, M. Asada, and N. Suzuki, Jpn. J. Appl. Phys. **31**, 57, (1994).
- [2] T. Suemasu, Y. Kohno, W. Saitoh, N. Suzuki, M. Watanabe, and M. Asada, Jpn. J. Appl. Phys. **33**, 1762 (1994).
- [3] K. Akai, M. Matsuura, Phys. Rev. **B60**, 5561(1999).
- [4] T. Kado, Journal of Appl. Phys. **78**, 3149 (1995).
- [5] T. Kado *et al.*, private communication.
- [6] T. Kado, K. Nakamura, M. Matsuura, THIN SOLID FILMS **545** (1999).
- [7] C. Strahberger, P. Vogl, Phys. Rev. **B62**, 7289 (2000).
- [8] J. P. Perdew, S. Burke, and M. Ernzerhof, Phys. Rev. Lett. **77**, 3865 (1996).
- [9] M. Murayama and T. Nakayama, J. Phys. Soc. Jpn. **61**, 2419 (1992).
- [10] J. J. Sakurai, Modern Quantum Mechanics, Addison-Wesley (New York, 1985), p. 337.